

On the nature of the X–ray absorption in the Seyfert 2 galaxy NGC 4507

A. Comastri¹ \star , C. Vignali², M. Cappi^{3,4}, G. Matt⁵, R. Audano², H. Awaki⁶, S. Ueno⁷

¹ Osservatorio Astronomico di Bologna, via Zamboni 33, I-40126 Bologna, Italy

² Dipartimento di Astronomia, Università di Bologna, via Zamboni 33, I-40126 Bologna, Italy

³ Istituto per le Tecnologie e Studio Radiazioni Extraterrestre/CNR, via Gobetti 101, I-40129 Bologna, Italy

⁴ The Institute for Physical and Chemical Research RIKEN, Wako-shi, Saitama 351-01, Japan

⁵ Dipartimento di Fisica, Università degli Studi ‘Roma Tre’, via della Vasca Navale 84, I-00146 Roma, Italy

⁶ Department of Physics, Faculty of Science, Kyoto University, Sakyo-ku, Kyoto 606-01, Japan

⁷ X-ray Astronomy Group, Department of Physics & Astronomy, University of Leicester, Leicester, LE1 7RH, U.K.

Received June 30; accepted October 27, 1997

ABSTRACT

We present results of the *ASCA* observation of the Seyfert 2 galaxy NGC 4507. The 0.5–10 keV spectrum is rather complex and consists of several components: (1) a hard X–ray power law heavily absorbed by a column density of about $3 \times 10^{23} \text{ cm}^{-2}$, (2) a narrow Fe $K\alpha$ line at 6.4 keV, (3) soft continuum emission well above the extrapolation of the absorbed hard power law, (4) a narrow emission line at ~ 0.9 keV. The line energy, consistent with highly ionized Neon (Ne IX), may indicate that the soft X–ray emission derives from a combination of resonant scattering and fluorescence in a photoionized gas. Some contribution to the soft X–ray spectrum from thermal emission, as a blend of Fe L lines, by a starburst component in the host galaxy cannot be ruled out with the present data.

Key words: galaxies: active – galaxies: individual: NGC 4507 – galaxies: Seyfert – X–rays: galaxies

1 INTRODUCTION

Studies of X–ray spectra of Seyfert 2 galaxies above a few keV (Awaki & Koyama 1993; Salvati et al. 1997) have revealed the presence of highly obscured nuclei with power law spectra and Fe $K\alpha$ lines similar to Seyfert 1 objects lending further support to the popular ‘Unification’ models for Active Galactic Nuclei (AGNs) (Antonucci 1993 and references therein). In these models the viewing angle explains most of the observed differences among Seyfert 1 and Seyfert 2 galaxies in terms of absorption by circumnuclear matter, possibly a molecular torus. If the orientation is such that the line of sight intercepts the torus, the Optical/UV radiation including the Broad Lines as well as the soft X–rays from the nucleus are blocked and the object is classified as a type 2. A fraction of the order of a few percent of the nuclear radiation can be detected in scattered light, the scattering medium being a warm plasma visible to both the nucleus

and the distant observer. The origin and the physical state of such a reflecting mirror are poorly known at present; this is unfortunate, as the mirror is a key component of the Unified model (Krolik & Kallman 1987) and several features originating from it are expected in X–rays (Krolik & Kriss 1995; Matt, Brandt & Fabian 1996), which should be observable at energies where the torus completely blocks the nuclear radiation. However, despite extensive studies of Seyfert 2 galaxies with *ROSAT* in the soft X–ray band (Mulchaey et al. 1993; Turner et al. 1993) the relatively low spectral resolution of the PSPC and the weakness of Seyfert 2 galaxies in the 0.1–3.0 keV energy range hampered detailed investigations of the soft component.

NGC 4507 is a nearby ($z = 0.011$) barred spiral galaxy, it was classified as a SBab(rs)I by Sandage & Brucato (1979). Optical spectra of the nucleus show emission lines characteristic of a Seyfert 2 type without any detectable broad line component (Durret & Bergeron 1986). The relatively high luminosity in the O [III] line ($\sim 6.5 \times 10^{41} \text{ ergs s}^{-1}$; Mulchaey et al. 1994), which is thought to be a good indicator of the luminosity of the Active Nuclei, suggests the

\star Andrea Comastri (comastri@astbo3.bo.astro.it)

presence of a powerful source of ionizing radiation. NGC 4507 is also a very bright far infrared source with a 60–100 μm luminosity derived from *IRAS* fluxes of $\sim 10^{44}$ ergs s^{-1} . In soft X-rays NGC 4507 is rather faint and only a marginal detection with the *Einstein* IPC has been reported (Fabbiano, Kim & Trinchieri 1992). At higher energies ($E > 3$ keV) it is a bright X-ray source and has been observed by several X-ray missions. A *Ginga* observation revealed a hard power law with a flat slope ($\Gamma_{2-20\text{keV}} \sim 1.4 \pm 0.2$), a high column density ($N_{\text{H}} \sim 3.7 \pm 0.5 \times 10^{23}$ cm^{-2}) and a strong iron emission line ($\text{EW} \sim 400 \pm 100$ eV) (Awaki et al. 1991; Smith & Done 1996). OSSE observations (Bassani et al. 1995) showed a steeper photon index $\Gamma \sim 2.1 \pm 0.3$ in the 50–200 keV energy range in agreement with those of Seyfert 1 galaxies in the same energy range (Johnson et al. 1994).

Here a 40 ksec *ASCA* observation of this bright Seyfert 2 galaxy is presented with the aim of a better understanding of the soft-to-medium X-ray emission.

Throughout the paper a Hubble constant $H_0 = 50$ $\text{Km s}^{-1} \text{Mpc}^{-1}$ and a deceleration parameter $q_0 = 0$ are assumed.

2 ASCA OBSERVATIONS AND DATA REDUCTION

NGC 4507 was observed with the Gas Imaging Spectrometer (GIS) and the Solid State Spectrometer (SIS) onboard the *ASCA* satellite (Tanaka, Inoue & Holt 1994) over the period 1994 February 12–13. The SIS data were obtained using 2-CCD readout mode, where 2 CCD chips are exposed on each SIS with the target at the nominal position. The source position in SIS1 was slightly offset from the nominal value. For this reason a fraction of the order of 20–30 per cent of the source flux was lost in the gap between the chips. Following a software-related problem on board *ASCA* the data collected from the GIS3 were corrupted. As they could not be easily recovered, they were therefore excluded from the analysis. In the following with GIS we refer to GIS2 data only.

All the SIS data were collected in FAINT telemetry mode, which maximises the CCD spectral resolution. The following criteria have been applied for the selection of good times intervals: the spacecraft was outside the South Atlantic Anomaly, the elevation angle from the Earth’s limb was > 5 degrees, the minimum bright Earth angle was > 25 degrees, the magnetic cutoff rigidity was greater than 6 GeV c^{-1} for SIS data and greater than 7 GeV c^{-1} for GIS data. ‘Hot’ and flickering pixels were removed from the SIS data, and rise-time rejection was applied to exclude particle events for the GIS data. SIS grades 0,2,3 and 4 were considered for the analysis. Finally a short period of unstable pointing at the phase of target acquisition was removed manually. After applying the above selection criteria, 25 ks for each SIS and 40 ks for the GIS detector were collected.

We fit the GIS and SIS data above 3 keV with an absorbed power law plus a narrow Gaussian line. The best fit energies in the three instruments are in good agreement. Since the gain of SIS and GIS were within 1 per cent of their nominal values, the source spectrum can be considered substantially not affected by instrumental gain offset.

NGC 4507 is clearly detected in all instruments together with a nearby (~ 6 arcmin) bright ($V = 5.8$) A0V star. In

the SIS0 the star is detected at the edge of the other CCD chip while is barely visible in the SIS1. Moreover the gap between the two chips prevents from a significant contamination. In order to estimate the possible contamination in the GIS field we have analysed the star spectrum. A thermal Raymond–Smith model ($kT \sim 1$ keV) provides a good fit to the data with some evidence of excess flux at higher energies suggesting that contamination effects between the two sources may be relevant. For this reason we have considered in the subsequent GIS analysis only counts at energies greater than 3 keV. Circular extraction cells of radius ~ 3.5 arcmin for SIS and ~ 4 arcmin for GIS centered on NGC 4507 were used, with corresponding background regions defined in source-free areas of the same CCD chip for SIS and from calibration background regions (blanksky) for GIS.

The background subtracted count rates for NGC 4507 are: 0.113 ± 0.002 cts s^{-1} and 0.081 ± 0.002 cts s^{-1} in SIS0 and SIS1, respectively (0.4–10 keV); 0.097 ± 0.002 cts s^{-1} in GIS in the 3–10 keV band.

3 RESULTS

Source plus background light-curves were accumulated for all the instruments showing no clear evidence for variability. GIS and SIS spectra were binned with more than 20 counts per bin in order to apply χ^2 statistics. The response matrices, effective areas and XRT PSF used were those released with the latest version of FTOOLS (3.6). Since the spectral parameters obtained by fitting an absorbed power law plus a soft component to the SIS0 and SIS1 spectra were all consistent at the ~ 90 per cent level and the residuals from those fits were very similar, we have added the two SIS spectra. In the overlapping energy range (3–10 keV) the GIS spectrum is consistent with the SIS results except for a slight mismatch (< 10 per cent) in the relative normalizations. In the following the spectral results are referred to the combined SIS0+SIS1 spectrum simultaneously fitted with the GIS2 one, leaving the relative normalizations free to vary. Unless explicitly stated all the quoted errors correspond to 90 per cent confidence intervals for one interesting parameter ($\Delta\chi^2 = 2.71$).

The continuum emission requires at least two components: an heavily absorbed hard X-ray power law at high energies and a soft component below ~ 3 keV. However, this model does not provide an adequate fit to the data. Two line-like excesses are clearly visible in the data/model ratio around 6.4 keV, indicative of iron $K\alpha$ emission (a feature commonly seen in Seyfert galaxies, Nandra & Pounds 1994; Mushotzky et al. 1995; Nandra et al. 1997) and around 0.9 keV, whose possible origin will be discussed later on. Moreover, strong deviations are present in the 1–3 keV region (Fig. 1). In the following subsections we provide a detailed description of the spectral complexity of NGC 4507.

3.1 The hard X-ray component

The hard X-ray spectrum is well fitted by an absorbed ($N_{\text{H}} \sim 10^{23.5}$) power law model plus a narrow Fe $K\alpha$ line, whose rest energy ($E = 6.36 \pm 0.03$ keV) indicates emission from neutral matter. The line EW (190 ± 40 eV) is consistent with the mean value of Seyfert 1 galaxies (Nandra et

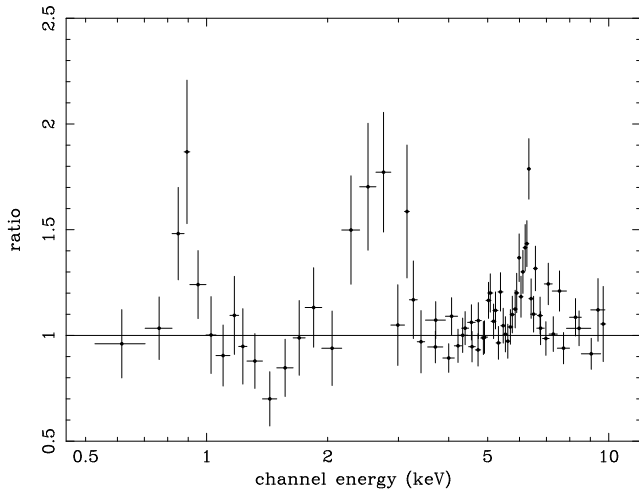


Figure 1. Data to model ratios in the 0.4–10 keV energy range for a model consisting of an absorbed power law at high energies plus a power law component at low energies. The Fe K line at 6.4 keV, a soft line at 0.9 keV and residuals in the 1–3 keV band are clearly visible.

al. 1997). The power law photon index is somewhat dependent on the precise spectral model chosen for the broad band spectrum. Fitting the data in the 3–10 keV energy range we obtain a best fit value of $\Gamma = 1.61 \pm 0.20$, which lies at the flatter end of the Seyfert 1 photon index distribution, which is characterized by an average value of $\Gamma \simeq 1.9$ (Nandra & Pounds 1994; Nandra et al. 1997). A reflection component has been added to the primary power law spectrum; however, given the relatively low effective area of *ASCA* above 6–7 keV, its amplitude is unconstrained by the present data and will not be further considered. A summary of spectral parameters is reported in Table 1.

3.2 The spectrum over the full energy range

The whole spectrum was then fitted using an absorbed power law plus iron line as a baseline model for the high energy spectrum, while several different models were fitted to the low energy spectrum. In all cases the absorption by our own Galaxy has been fixed at the value of $N_{HGal} = 7.19 \times 10^{20} \text{ cm}^{-2}$ (Dickey & Lockman 1990). The results are reported in Table 2.

Simple thermal models (Bremsstrahlung and Raymond–Smith) for the soft component do not provide good fits leaving strong residuals at all energies below 3 keV. A steep $\Gamma = 2.43 \pm 0.22$ power law model for the soft X-ray band gives instead a better description of the data, with a relative normalization with respect to the hard power law of ~ 2 per cent; however, also in this case, the fit is rather poor (Table 2), since two remarkable structures appear in the residuals: a line-like feature around 0.9 keV and a waving behaviour in the 1–3 keV range with an ‘hump’ between 2 and 3 keV (Fig. 1). It appears clear that a single power law for the soft X-ray spectrum which could be interpreted as the fraction of the direct continuum emission which is scattered into our line of sight by the reflecting mirror is a too simple an approximation. The addition of a narrow line

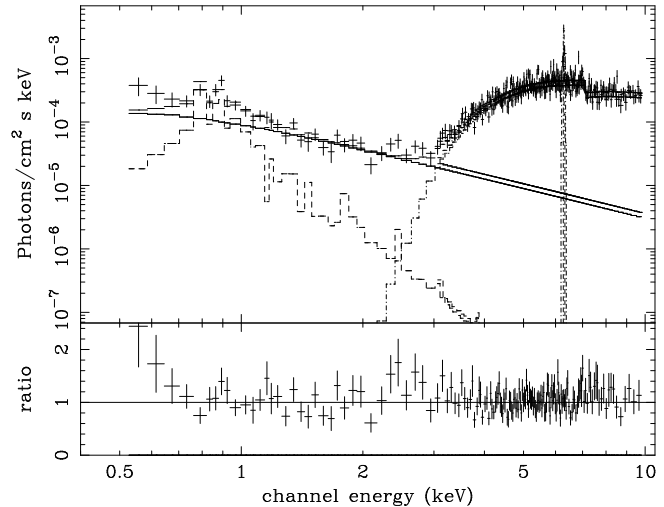


Figure 2. The NGC 4507 unfolded spectrum, fitted with an absorbed power law plus Fe K line at high energies, plus a scattered power law and Raymond–Smith thermal emission for the soft energy range (upper panel). Data to model ratio is shown in the lower panel.

gives a significant improvement ($\Delta\chi^2 \simeq 19$) with a best fit line energy of 0.90 ± 0.02 keV and $EW \sim 140 \pm 50$ eV.

The slope of the low energy power law is steeper than the hard one and would be inconsistent with a simple scattering model. However the soft X-ray nuclear spectrum scattered into our line of sight could be intrinsically steeper because affected by the soft excess frequently observed in Seyfert 1 galaxies. If the soft photon index is forced to be the same of the hard one the fit is slightly worse as some flux excess is present in the 0.5–0.7 keV region. A possible interpretation of this excess as a blend of unresolved oxygen lines is discussed below.

An inherent limitation of the *ASCA* data is that the complexity of the spectrum in terms of absorption and emission lines features hampers a precise estimate of the spectral slope. For this reason in the following we assume that the slope of the scattered power law is equal to the hard one ($\Gamma_s \equiv \Gamma_h$).

A combination of a thermal model and a power law for the soft spectrum clearly improves the fit owing to the greater number of free parameters. The derived temperature for the thermal component ($kT \sim 0.7 \pm 0.1$ keV) is much lower than the typical values derived for late type galaxies ($kT \sim 3$ –5 keV; Kim, Fabbiano & Trinchieri 1992) such as NGC 4507, but consistent with the characteristic temperatures inferred from recent *ASCA* observations of starburst galaxies (Serlemitsos, Ptak & Yaqoob 1997). Leaving the abundances of the Raymond–Smith model free to vary there is no improvement in the fit. We note that, even with such a complex model, the line-like feature at 0.9 keV is not completely accounted for (unless Neon abundances are left free to vary) and, moreover, the residuals below ~ 0.8 keV are steeply increasing towards lower energies (Fig. 2).

The shape of the residuals below ~ 3 keV and the evidence of a line-like excess at ~ 0.9 keV suggests, instead (see below), that ionized absorption/reflection of the nuclear

Table 1. 3–10 keV Spectral Fits. ^a units of 10^{22} cm⁻²; ^b in keV; ^c in eV; ^d Total χ^2 and degrees of freedom.

Γ	N_{H}^a	E_{line}^b	EW ^c	χ^2/dof^d
1.78 (1.59–1.98)	32.4 (30.1–34.7)			363.8/278
1.61 (1.41–1.81)	29.2 (26.9–31.5)	6.36 (6.34–6.39)	189 (153–225)	296.9/276

Table 2. 0.5–10 keV Spectral Fits. ^a Hard Photon spectral index; ^b Cold absorption column density (units of 10^{22} cm⁻²); ^c Soft Photon spectral index; ^d Thermal models temperature (keV); ^e Abundances with respect to the Solar values; ^f Soft Line energy (keV); ^g Soft Line equivalent width (eV); ^h Total χ^2 and degrees of freedom.

Γ_h^a	N_{H}^b	Γ_s^c	kT^d	Z/Z_{\odot}^e	E_{line}^f	EW ^g	χ^2/dof^h
1.49 (1.32–1.67)	27.8 (26.1–29.9)	2.43 (2.21–2.65)	363.8/321
1.44 (1.27–1.63)	26.8 (24.6–28.8)	...	1.27 (0.94–1.72)	< 0.03	380.1/320
1.43 (1.27–1.62)	26.6 (24.8–28.6)	...	1.25 (1.08–1.65)	brems.	380.3/321
1.56 (1.40–1.71)	29.4 (27.7–31.0)	1.56 ($\equiv \Gamma_h$)	0.71 (0.62–0.79)	1 (f)	346.3/320
1.52 (1.34–1.71)	28.4 (26.3–30.5)	2.14 (1.86–2.40)	0.90 (0.88–0.91)	140 (89–192)	345.2/319
1.74 (1.59–1.88)	31.2 (29.7–32.7)	1.74 ($\equiv \Gamma_h$)	0.90 (0.88–0.92)	211 (153–269)	352.1/320

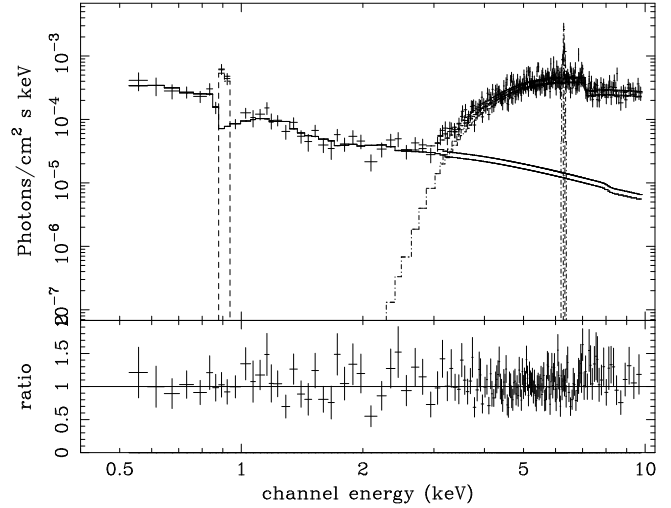
radiation by a warm scattering mirror could be important in the modelling of the soft X-ray spectrum.

It should be noted that the putative ionized absorber has significant effects only on the soft scattered component, while the hard X-ray emission is absorbed by almost neutral material as described in the previous section.

A composite cold plus warm absorber model has been fitted to the overall spectrum of NGC 4507 using the ABSORI model available in XSPEC 9.0. Given the relatively large number of free parameters of the warm absorber model we have fixed the temperature of the warm material at $T = 10^5$ K (the temperature dependence in this model is very weak in the range $T = 10^{4.5-5.5}$ K), the iron abundance at the solar value and the slope of the primary power law at the same value of the hard component as is expected if the soft emission is scattered into our line of sight by the warm mirror. The fitted parameters are thus the column density N_W of the warm gas and the ionization parameter ξ which are related by: $\xi = L/n_e R^2$. A summary of the derived values is reported in Table 3. It should be noted that such a model only describes the photoabsorption of a background X-ray source, while the case of NGC 4507 is possibly more complex owing to the different geometry and physical parameters of the scattering region (see below and § 4.2.1). For this reason ABSORI should be considered as a first order approximation for the description of the soft X-ray continuum in NGC 4507.

With such a model the waving structure in the 1–3 keV range can be almost entirely accounted for by the characteristic absorption features of warm gas the only remaining feature is a strong line at ~ 0.9 keV. A highly significant improvement (at > 99.99 per cent according to an F-test) has been obtained by adding a narrow gaussian line with EW ~ 370 eV and ~ 1.3 keV with respect to the unabsorbed (Fig. 3) and absorbed continuum, respectively, the latter value in agreement with the calculations by Netzer (1996).

The line energy ($E = 0.92 \pm 0.02$ keV) is consistent

**Figure 3.** The best fitting unfolded spectrum. The hard component is fitted with an absorbed power law plus Fe K line at 6.4 keV. The soft component is represented by a warm absorbed power law continuum plus a line at 0.92 keV (upper panel). Data to model ratio is shown in the lower panel.

with Ne IX and may be produced in the photoionized gas with contributions from both the resonant scattering and recombination emission (Matt et al. 1996). The relative contribution of the two components depends strongly on the optical depth of the emitting matter, and will be discussed in the next section. We note that the Ne IX line is among the most prominent features predicted in the warm absorber model of Netzer (1996; see his Fig. 4), owing to the relatively high abundance of Neon and to the large continuum absorption of ionized gas around 0.8–0.9 keV.

An alternative possibility for the line-like emission at 0.9 keV is in terms of thermal emission from a hot thin

Table 3. 0.5–10 keV Spectral Fits with warm absorber. ^a Photon spectral index; ^b Cold absorption column density (units of 10^{22} cm⁻²); ^c Warm absorption column density (units of 10^{22} cm⁻²); ^d Ionization parameter in ergs cm s⁻¹; ^e Thermal models temperature (keV); ^f Soft Line energy (keV); ^g Soft Line equivalent width (eV) with respect to the unabsorbed continuum; ^h Total χ^2 and degrees of freedom.

Γ_h^a	N_H^b	N_W^c	ξ^d	kT^e	E_{line}^f	EW^g	χ^2/dof^h
1.89 (1.79–2.02)	33.6 (32.2–35.1)	8.5 (4.3–14.2)	731 (467–1178)	369.3/320
1.64 (1.46–1.81)	31.4 (29.6–33.1)	8.3 (2.6–20.6)	520 (220–1194)	0.82 (0.69–0.92)	338.4/318
1.74 (1.62–1.86)	32.6 (31.2–33.4)	12.0 (6.1–19.7)	780 (472–1393)	...	0.92 (0.90–0.93)	372 (216–612)	333.8/318

plasma, possibly associated with a starburst component, is also viable. The improvement with respect to a fit with a warm absorber model for the soft spectrum is significant (see Table 3) even if this fit is not as good as the one with a narrow line at 0.9 keV ($\Delta\chi^2 \sim 5$). Leaving the abundances of the Raymond–Smith model free to vary there is no improvement in the fit quality.

We find a significantly larger ionized column density and ionization parameter with respect to the average properties of the warm absorbers in Sey 1s ($\langle \xi \rangle \sim 30$ ergs cm s⁻¹, $\langle N_W \rangle \sim$ a few $\times 10^{21}$ cm⁻², Reynolds 1997). The larger N_W is required from the fitting to account for the spectral behaviour in the ~ 1.5 –3 keV energy range (Fig. 1). As a consequence, a greater ξ is needed to account for the data below ~ 1.5 keV. We note, however, that these values do not necessarily require a different ionization structure between NGC 4507 and Sey 1s, but can be explained with a higher inclination angle (i.e. a ‘warm scattering mirror’ rather than a ‘warm absorber’). It’s interesting to note that even larger values for N_W and ξ have been recently reported for the Sey 2 galaxy Mkn 3 (Turner et al. 1997).

4 DISCUSSION

4.1 The obscured nucleus

The high energy (> 3 keV) power law slope is relatively flat, but consistent with a typical Seyfert 1 spectrum. The absorption column density, spectral slope and flux level are consistent with the previous *Ginga* observation, without any evidence of flux and/or spectral variability over a timescale of about 4 years (Awaki et al. 1991; Smith & Done 1996). On the other hand the source was a factor 2 brighter in the 2–10 keV band during the 1984 *EXOSAT* observation (Polletta et al. 1996).

The observed 2–10 keV flux of the hard power law component is 2.1×10^{-11} ergs cm⁻² s⁻¹, corresponding to an absorption corrected luminosity of 3.7×10^{43} ergs s⁻¹, which is within the range of Seyfert 1 nuclei.

A comparison of the best-fit spectral parameters for the hard component with the previous *Ginga* values (Awaki et al. 1991, Smith & Done 1996) suggests a possible variation of the Fe $K\alpha$ line intensity and, eventually, of the absorption column density. However, given the uncertainties due to the lower energy resolution of *Ginga* and in the cross-calibration of the two instruments, firm conclusions on this issue cannot be drawn.

With the present constraints, the Fe $K\alpha$ emission line intensity is consistent with transmission trough cold matter with

a column density of a few 10^{23} cm⁻² (Awaki 1991; Ghisellini, Haardt & Matt 1994), though the data do not rule out some contribution from a reflection component in the continuum and in the line.

4.2 The soft component

4.2.1 Contribution from ionized gas

The evidence of highly ionized material that leaves significant imprints on the 0.1–10 keV spectrum of Seyferts galaxies and quasars is by now widely recognized and, thanks to the *ASCA* capabilities, ‘warm absorbers’ have been clearly detected in several Seyfert 1 and quasars (Fiore et al. 1993; Otani et al. 1996; Reynolds 1997). Several theoretical models have been developed to explain the observed features (e.g. Netzer 1996 and references therein).

When the ionized gas lies on the line of sight, as for Seyfert 1 objects, absorption features of the oxygen edges at 0.74 and 0.87 keV are usually the most evident characteristics, while the strongest lines when observed against the direct continuum have typical equivalent widths of a few tens of eV at most, so that are difficult to detect with the present detectors. Much larger equivalent widths for the emission lines are expected if the central continuum source is obscured as in the case of Seyfert 2 galaxies (e.g. Netzer 1996).

We therefore interpret the observed feature around 0.9 keV we have detected in the spectrum of NGC 4507 as an emission line (parametrized as a gaussian) from warm material out of the line of sight, i.e. the same material responsible for the scattering of the continuum. In figures 4 and 5 the contour plots of the line energy vs. normalization (with the line width set to zero) and vs. the width (when permitted to vary) are shown. The best fit line energy suggests the identification of this feature with $K\alpha$ emission from He-like Neon (0.92 keV). If the reflecting matter would be optically thin to all processes, the expected EW would be (see Matt et al. 1996 for the relevant formulae) about 6 keV (assuming solar abundances and a fraction of Ne IX of 0.4–0.5), resonant scattering accounting for about 90 per cent of it, to be compared with an observed EW of more than one order of magnitude smaller (Table 2 and 3). However, matter becomes optically thick to resonant scattering when $N_H \sim$ a few 10^{19} and to photoabsorption when $N_H \sim 10^{23}$ at the edge energy, and at a value five times smaller at the line energy. Because for these values of the column density Compton scattering is still optically thin, line EWs are largely dimmed (Matt et al. 1996). If the N_H is actually of order of 10^{23} , as suggested by the amount of scattered continuum photons, equivalent

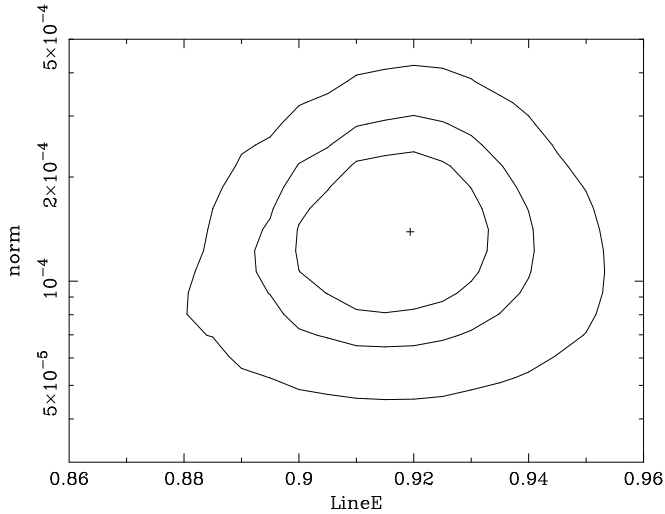


Figure 4. Confidence contour levels (68, 90 and 99 per cent) for two interesting parameters: line energy and flux.

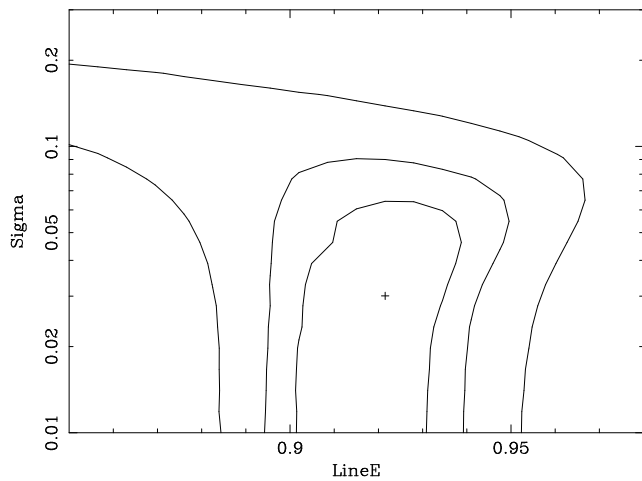


Figure 5. Confidence contour levels (68, 90 and 99 per cent) for two interesting parameters: line energy and width.

widths of the order of the observed one can be attained. A further reduction in the line strength arises from the fact that the line or, better, the resonant and intercombination lines, is resonantly trapped in the medium and may be eventually destroyed by photoabsorption by an Oxygen atom. The exact value of the line EW depends on several physical and geometrical details, and its precise evaluation is beyond the scope of this paper. Note that a strong He-like oxygen line at 0.57 keV is also to be expected. Unfortunately, the SIS efficiency at that energy is rather poor and prevents a detailed study of this feature; in any case, the obtained upper limit of $O/Ne \sim 4-5$ is consistent with the expectation.

Another possible explanation for the ~ 0.9 keV feature is in term of recombination on ground state of completely stripped oxygen, following a photoionization of an O VIII atom. The threshold energy is 0.87 keV, which is inconsistent at the 3σ level with the observed line energy (Fig. 4).

However, the recombination feature should have a line-like appearance only if the temperature of the matter is much lower than the threshold energy; but with a temperature of 10^6 K, not impossible in photoionized plasma, the width of the feature should be not negligible and still consistent with the observation (Fig. 5), with the centroid energy shifted towards higher energy. Assuming, as usual, photoionized plasma, the expected EW in the optically thin case is (for solar abundances and a fraction of O VIII of 0.4-0.5) about 2 keV. Again, this EW diminishes with the column density, and again values similar to that observed can be obtained for columns of the order of 10^{23} cm^{-2} . In this case a recombination line at 0.65 keV from O VIII, with a similar equivalent width, is also to be expected. The obtained 90 per cent upper limit to such a line is about 50 eV. At these column densities, however, such a line got resonantly trapped and may be eventually destroyed by photoabsorption by for example C VI, which may help explaining the low intensity of this line with respect to the recombination continuum. Obviously a final possibility is that both Ne IX and the O VIII lines can contribute to the observed emission. In fact, despite the fact that the ionization potentials of Ne VIII and O VII are quite different (as in the last ion the ionization should involve a K instead than L electron), it is possible to have both ions rather abundant at the same time (see e.g. Nicastro et al. 1997).

With the values of the column density of the warm matter as derived by both the amount of reflected continuum and the equivalent width of the 0.9 keV feature (whatever its origin), a substantial re-absorption of the scattered photons is expected. As the matter responsible for both the photons emission and absorption is the same, the adoption, for the fitting procedure, of a warm screen in front of the line and continuum emitting region, as we have done in the previous section, may be not completely appropriate to the physical situation under investigation. A self-consistent grids of models taking into account also emission and reflection processes in ionized plasmas, such as those computed using e.g. CLOUDY or XSTAR would probably be more appropriate. We note, however, that the physical picture obtained using ABSORI plus a Gaussian line at ~ 0.9 keV is in overall good agreement with much more detailed calculations (Krolik & Kriss 1995; Netzer 1996), and that, in any case, the quality of the data is not such to permit an unambiguous determination of all the parameters.

Interestingly, the derived value of the absorbing column density is of the same order of that derived for the reflector, giving a check of our hypothesis that the reflector and the absorber are one and the same material. The line EW is now somewhat greater, but of the same order of magnitude, than in the previous case. The best fit ionization structure of the absorbing matter suggests that H-like oxygen and neon ions are dominating over He-like ions, consistent with the O VIII recombination line hypothesis for the 0.9 keV feature. Observations with instruments with higher energy resolution and sensitivity, like AXAF, XMM and ASTRO-E, are clearly requested to clarify this issue.

4.2.2 Contribution from the starburst

Galaxies where the star formation rate greatly exceed the average rate of normal galaxies are called starburst galax-

ies. Their optical spectra are characterized by intense narrow emission lines due to a recent episode of star formation and strong infra-red emission probably due to dust reprocessing of the radiation from hot stars. Shock-heated gas is expected to emit in the X-ray band with luminosities a few order of magnitude lower than those usually observed for Seyfert galaxies (see Serlemitsos et al. 1997 for a recent review) However when the emission of the AGN is obscured as in the case of Seyfert 2 galaxies the starburst component could provide an important contribution to the soft X-ray emission. An estimate of the expected X-ray luminosity from the starburst component can be obtained from the far infrared luminosity (David, Jones & Forman 1992).

Given a FIR luminosity of NGC 4507 of $\sim 1.1 \times 10^{44}$ ergs s^{-1} the expected 0.5–4.5 keV luminosity is $\sim 7.8 \times 10^{40}$ ergs s^{-1} (equation 1 in David et al. 1992), while the observed luminosity of the soft component in the same energy band is $\sim 2.2 \times 10^{41}$ ergs s^{-1} , i.e. about a factor three greater. This result suggests that the thermal component may account only for a relatively small fraction (< 30 per cent) of the observed soft X-ray luminosity.

Previous *ROSAT* and *ASCA* observations of starburst galaxies (i.e. Makishima et al. 1994; Moran & Lehnert 1997) have shown that the soft X-ray emission below 2 keV is frequently extended over a region greater than 1 arcmin in extent. A pointed PSPC observation of NGC 4507 has been retrieved from the public archive. The source is rather weak with an observed 0.5–2.0 keV flux of $\sim 3 \times 10^{-13}$ ergs cm^{-2} s^{-1} consistent with the value derived from our *ASCA* analysis in the same energy range. The image is consistent with a pointlike source at the PSPC spatial resolution of ~ 25 arcsec to be compared with the extent of the optical image ($\sim 1.3 \times 1.7$ arcmin). The lack of any extended emission and the spectral analysis results indicate that the contribution of a starburst component, if present, plays a minor role for explaining the soft X-ray emission of NGC 4507.

5 SUMMARY

The main results of the *ASCA* observation of the bright Seyfert 2 galaxy NGC 4507 can be summarized as follows:

- The hard (> 3 keV) power law slope ($\Gamma \simeq 1.4$ – 1.8) lies at the flatter-end of the Seyfert 1 photon index distribution. The continuum is strongly absorbed at few keV by a column density $N_H \simeq 3 \times 10^{23}$ cm^{-2} . The iron line intensity (EW $\simeq 190 \pm 40$ eV) is consistent with transmission through cold matter with such a column density.

- The soft X-ray spectrum is rather complex and cannot be approximated with a single component. A scattered power law plus emission from hot thermal gas provide an acceptable description of the soft X-ray continuum, but several features are left in the residuals. A thermal component possibly due to a starburst would in any case account for < 30 per cent of the soft X-ray flux.

- Reflection and self-absorption in a photoionized plasma provide a better description of the overall soft X-ray spectrum. A line feature at 0.9 keV is clearly detected, probably due to the Ne IX $K\alpha$ recombination, even if some contribution from the O VIII recombination continuum cannot be excluded. Note that the presence of visible soft emission line in Seyfert 2's are expected (Matt et al. 1996; Netzer

1996), and have probably already been detected by *ASCA* in other Seyferts like Mkn 3 (Iwasawa et al. 1994), NGC 4051 (Guainazzi et al. 1996) and NGC 4388 (Iwasawa et al. 1997), as well as in the well known Seyfert 1.5 NGC 4151 (Leighly et al. 1997).

A broad band observation over the full X-ray domain from 0.1 to several tens of keV, like that will be performed by BeppoSAX, would allow a better estimate of the relative contribution of the scattered radiation from the warm gas and the starburst component. A more detailed study of the warm absorption/reflection requires good energy resolution and sensitivity; *AXAF*, *XMM* and *ASTRO-E* will surely improve significantly our understanding of these phenomena.

ACKNOWLEDGEMENTS

AC acknowledges financial support from the Italian Space Agency under the contract ASI-95-RS-152. We thank an anonymous referee for useful comments. This work has made use of the NASA/IPAC Extragalactic Database (NED) which is operated by the Jet Propulsion Laboratory, Caltech, under contract with the National Aeronautics and Space Administration.

REFERENCES

- Antonucci R.R.J., 1993, *ARA&A*, 31, 473
 Awaki H., 1991, PhD Thesis, University of Nagoya
 Awaki H., Koyama K., 1993, *Adv. Space Res.*, 13, 221
 Awaki H., Kunieda H., Tawara Y., Koyama K., 1991, *PASJ*, 43, L37
 Bassani L., Malaguti G., Jourdain E., Roques J.P., Johnson W.N., 1995, *ApJ*, 444, L73
 David L.P., Jones C., Forman W., 1992, *ApJ*, 388, 82
 Dickey J.M., Lockman F.J., 1990, *ARA&A*, 28, 215
 Durret F., Bergeron J., 1986, *A&A*, 156, 51
 Fabbiano G., Kim D.-W., Trinchieri G., 1992, *ApJS*, 80, 531
 Fiore F., Elvis M., Mathur S., Wilkes B., McDowell J., 1993, *ApJ*, 415, 129
 Ghisellini G., Haardt F., Matt G., 1994, *MNRAS*, 267, 743
 Guainazzi M., Mihara T., Otani C., Matsuoka M., 1996, *PASJ*, 48, 781
 Iwasawa K., Yaqoob T., Awaki H., Ogasaka Y., 1994, *PASJ*, 46, L167
 Iwasawa K., Fabian A.C., Ueno S., Awaki H., Fukazawa Y., Matsushita K., Makishima K., 1997, *MNRAS*, 285, 683
 Johnson W.N. et al., 1994, in Fichtel C.E., Gehrels N., Norris J.P., eds, *Proc. of The Second Compton Symposium*, AIP Vol. 304, p. 515
 Kim D.W., Fabbiano G., Trinchieri G., 1992, *ApJ*, 393, 134
 Krolik J.H., Kallman T.R., 1987, *ApJ*, 320, L5
 Krolik J.H., Kriss G.A., 1995, *ApJ*, 447, 512 (erratum in 1996, *ApJ*, 456, 909)
 Leighly K.M., Cappi M., Matsuoka M., Mihara T., 1997, in Makino F., Mitsuda K., eds, *X-ray Imaging and Spectroscopy of Cosmic Hot Plasmas*, University Academy Press, Tokyo, p. 291
 Makishima K. et al., 1994, *PASJ*, 46, L77
 Matt G., Brandt W.N., Fabian A.C., 1996, *MNRAS*, 280, 823
 Moran E.C., Lehnert M.D., 1997, *ApJ*, 478, 172
 Mulchaey J.S., Colbert E., Wilson A.S., Mushotzky R.F., Weaver K.A., 1993, *ApJ*, 414, 144
 Mulchaey J.S., Koratkar A., Ward M.J., Wilson A.S., Whittle M., Antonucci R.R.J., Kinney A.L., Hurt T., 1994, *ApJ*, 436, 586

- Mushotzky R.F., Fabian A.C., Iwasawa K., Kunieda H., Matsuoka M., Nandra K., Tanaka Y., 1995, MNRAS, 272, 9
Nandra K., Pounds K.A., 1994, MNRAS, 268, 405
Nandra K., George I.M., Mushotzky R.F., Turner T.J., Yaqoob T., 1997, ApJ, 477, 602
Netzer H., 1996, ApJ, 473, 781
Nicastrò F. et al., 1997, in preparation
Otani C., Kii T., Reynolds C.S. et al., 1996, PASJ, 48, 211
Polletta M., Bassani L., Malaguti G., Palumbo G.G.C., Caroli E., 1996, ApJS, 106, 399
Reynolds C.S., 1997, MNRAS, 286, 513
Salvati M., Bassani L., Della Ceca R., Maiolino R., Matt G., Zamorani G., 1997, A&A, 323, L1
Sandage A., Brucato R., 1979, AJ, 84, 472
Serlemitsos P., Ptak A., Yaqoob T., 1996, in Eracleous M., Koratkar A., Leitherer C., Ho L., eds, The Physics of LINERs in View of Recent Observations, p. 70
Smith D.A., Done C., 1996, MNRAS, 280, 335
Tanaka Y., Inoue H., Holt S.S. 1994, PASJ, 46, L37
Turner T.J., Urry C.M., Mushotzky R.F., 1993, ApJ, 418, 653
Turner T.J., George I.M., Nandra K., Mushotzky R.F., 1997, ApJ, in press